# Local Atomic Ordering in $BaTaO_2N$ Studied by Neutron Pair Distribution Function Analysis and Density Functional Theory

Katharine Page,[†] Matthew W. Stoltzfus,[‡] Young-Il Kim,[‡] Thomas Proffen,[§] Patrick M. Woodward,*[,‡] Anthony K. Cheetham,*[,†] and Ram Seshadri*[,†]

*Materials Department and Materials Research Laboratory, University of California, Santa Barbara, California 93106, Department of Chemistry, The Ohio State University, Columbus, Ohio 43210, and Los Alamos National Laboratory, Lujan Neutron Scattering Center, Lansce-12, MS H805, Los Alamos, New Mexico 87545*

*Received April 7, 2007. Revised Manuscript Received May 29, 2007*

The local structure and oxygen/nitrogen ordering of the high permittivity perovskite $BaTaO_2N$ has been studied using a combination of neutron total scattering and density functional electronic structure calculations. Although the average structure as revealed by neutron diffraction Rietveld analysis is cubic $Pm\bar{3}m$ with no evidence of O/N ordering, the local structure as revealed by pair distribution function analysis of the total neutron scattering appears to favor a cis configuration of the $TaO_4N_2$ polyhedra with small Ta displacements toward the N atoms. Density functional calculations similarly suggest that the cis $TaO_4N_2$ polyhedron is more stable than the corresponding trans variant.

## Introduction

The replacement of oxygen by nitrogen in transition metal oxides can have profound effects on the optical properties because the more covalent nature of the nitride anion results in decreased band gaps. Thus highly colored oxynitride compounds have been proposed as candidate replacements for many heavy-metal-containing pigments.[1] The unique electronic properties make oxynitride compounds promising as photocatalysts as well.[2] The increased cation−anion covalency in oxynitrides might equally be expected to influence dielectric properties.

There has been considerable interest recently in perovskite oxynitrides, the group of compounds formed by partial replacement of oxygen by nitrogen in $ABO_3$ perovskites.[3−8] In these materials, the increase in negative charge upon replacing O by N is compensated by simultaneously replacing the B cation by metals with higher cationic charge. Thus compounds that are electronically equivalent to $d^0$ perovskites such as $BaTiO_3$ and $BaZrO_3$ can be envisaged, for example, as corresponding to $BaNbO_2N$ and $BaTaO_2N$.

The preparation of $BaTaO_2N$ was first reported by Marchand et al.[3] More recently the dielectric properties of $BaTaO_2N$ were measured by Kim et al.[9,10] and found to be rather unusual: Polycrystalline $BaTaO_2N$ has a relative bulk permittivity in excess of 4500, with a moderate temperature coefficient, 1140 ppm $K^{-1}$, near room temperature, whereas epitaxially grown $BaTaO_2N$ thin films are found to possess a permittivity in the range of 200−240 with a temperature coefficient of −50 to −100 ppm $K^{-1}$. The compound is very stable in air, water, and acids and contains relatively nontoxic elements, all of which make it promising for applications. Materials with such high permittivities are frequently associated with polar behavior and often display phase transitions to lower-symmetry structures. It is therefore somewhat surprising that neutron,[4] X-ray,[9] and electron[9] diffraction of polycrystalline $BaTaO_2N$ all suggest the cubic $Pm\bar{3}m$ space group and show no evidence for O/N ordering. Neither does temperature-dependent X-ray diffraction suggest a phase transition at low temperatures.[9]

Fang et al.[11] have reported density functional electronic structure calculations on $BaTaO_2N$ with specific regard to its local structure. Both cis and trans arrangements of N in $TaO_4N_2$ octahedra were found by DFT to support formation of local dipoles. The energy of a cis configuration was found to be about 0.2 eV (per $BaTaO_2N$ unit) lower than the energy of a trans arrangement. Disordered anion arrangements were found to be slightly favored energetically, although the authors mention that choice of cell volume can bias what emerges as the preferred structural distortion.

* Corresponding author. E-mail: seshadri@mrl.ucsb.edu (R.S.).
[†] University of California, Santa Barbara.
[‡] The Ohio State University.
[§] Los Alamos National Laboratory.

(1) Jansen, M.; Letschert, H. P. *Nature* **2000**, *404*, 980−982.
(2) Kasahara, A.; Nukumizu, K.; Hitoki, G.; Takata, T.; Kondo, J. N.; Hara, M.; Kobayashi, H.; Domen, K. *J. Phys. Chem. A* **2002**, *106*, 6750−6753.
(3) Marchand, R.; Pors, F.; Laurent, Y.; Regreny, O.; Lostec, J.; Hausonne, J. M. *J. Physique* **1986**, *47* (*C-1*), 901−905.
(4) Pors, F.; Marchand, R.; Laurent, Y.; Bacher, P.; Roult, G. *Mater. Res. Bull.* **1988**, *23*, 1447−1450.
(5) Günther, E.; Hagenmayer, R.; Jansen, M. *Z. Anorg. Allg. Chem.* **2000**, *626*, 1519−1525.
(6) Clarke, S. J.; Guinot, B. P.; Michie, C. W.; Calmont, M. J. C.; Rosseinsky, M. J. *Chem. Mater.* **2002**, *14*, 288−294.
(7) Clarke, S. J.; Hardstone, K. A.; Michie, C. W.; Rosseinsky, M. J. *Chem. Mater.* **2002**, *14*, 2664−2669.
(8) Ebbinghaus, S. G.; Weidenkaff, A.; Rachel, A.; Reller, A. *Acta Crystallogr., Sect. C* **2004**, *60*, i91−i93.
(9) Kim, Y.-I.; Woodward, P. M.; Baba-Kishi, K. Z.; Tai, C. W. *Chem. Mater.* **2004**, *16*, 1267−1276.
(10) Kim, Y.-I.; Si, W.; Woodward, P. M.; Sutter, E.; Park, S.; Vogt, T. *Chem. Mater.* **2007**, *19*, 618−623.
(11) Fang, C. M.; de Wijs, J. A.; Orhan, E.; de With, G.; de Groot, R. A.; Hintzen, H. T.; Marchand, R. *J. Phys. Chem. Solids* **2003**, *64*, 281−286.

10.1021/cm0709673 CCC: $37.00 
Published on Web 07/17/2007

The local structure of $BaTaO_2N$ has previously been probed by extended X-ray absorption fine structure (EXAFS) at the Ta $L_3$-edge.[12] The nearest $Ta(O,N)_6$ shell from EXAFS appeared as a broad, bimodal peak in the radial distribution function, clearly indicating a low-symmetry coordination geometry around Ta. This bimodal peak character was not observed in the fourth shell and beyond ($r > 4.5$ Å), suggesting that any local ionic displacements occur with an extremely small correlation length. In the above EXAFS analysis, the Ta−O and Ta−N bonds could not be distinguished because of the very similar X-ray scattering from O and N. The question of whether N are cis or trans in the $TaO_4N_2$ octahedra similarly could not be addressed.

Here, we approach the problem of the local structure and O/N ordering of $BaTaO_2N$ using the pair distribution function (PDF) analysis of neutron total scattering data. The use of neutrons is particularly appropriate for the problem of O/N ordering because these elements are well-separated in terms of their scattering lengths, at 5.805 and 9.36 fm,[13] respectively. The ability of the PDF technique to extract short-range order from diffuse scattering components has been demonstrated by both simulation and experiment.[14]

Previous studies of polar materials have utilized the PDF technique to effectively probe local structural distortions. For example, Egami and co-workers have examined the relaxor ferroelectric $Pb(Mg_{1/3}Nb_{2/3})O_3$ (PMN) and found that the local structure of the compound determined by the PDF was markedly different than the average crystal structure.[15] The important piezoelectric system $Pb(Zr,Ti)O_3$ has also been examined using PDF methods by Egami et al.[16] Petkov et al.[17] have recently demonstrated the use of the PDF to understand local structure distortions and polar behavior in $Ba_xSr_{1-x}TiO_3$ nanocrystals. We present the average and local crystal structure of $BaTaO_2N$ as determined by the combination of Rietveld and PDF refinements of time-of-flight neutron powder diffraction data. We also present density functional calculations of the relative stabilities of the structural models that are employed in the PDF analysis.

Although no evidence for long range anion ordering has been seen in $BaTaO_2N$, there are some reports of anion ordering in oxynitride perovskites. Günther et al.[5] have reported the preparation of O/N ordered $SrTaO_2N$ in the *I*4/*mcm* space group. Their preparation involved the use of a halide mineralizer, believed to assist in the ordering. Ebbinghaus et al.[8] have reported ∼85%-ordered $SrNbO_2N$ also in the *I*4/*mcm* space group. However, although the $TaO_4N_2$ octahedra have trans N atoms in the former, the N atoms are largely cis in $SrNbO_2N$. Reports of ordered oxynitride perovskite compounds seem to be the exception rather than the rule. However, given how sensitively O/N ordering can depend on preparative conditions, it should be recognized that the structural results presented here may not be universally valid for all $BaTaO_2N$ samples.

## Experimental Section

In this study, we employed the same sample whose X-ray structure, dielectric properties, and electron diffraction were reported in the literature.[9] The sample was prepared by ammonolysis of mixed powders of $BaCO_3$ (J. T. Baker, 99.8%), and $Ta_2O_5$ (Cerac, 99.5%). The stoichiometric mixture was mixed in acetone using an agate mortar and pestle, placed in an alumina boat, and heated in flowing anhydrous ammonia (99.99%, ∼0.5 mL/s) to between 1223 and 1273 K at a rate of 5 K/min. After being held there for as long as 80 h, the mixture was cooled at 10 K/min.[9] The same sample was used in the EXAFS study.[12]

Time-of-flight neutron powder diffraction data were collected on the NPDF instrument at the Los Alamos National Laboratory Lujan Neutron Scattering Center[19] at room temperature. This instrument is capable of providing diffraction data out to high values of the wave vector $Q$, which is important for the employment of the PDF technique. Approximately 2 g of powder were loaded into a vanadium can for the experiment, and data were collected for 12 h. The diffraction data were analyzed with the Rietveld method as embodied in the GSAS-EXPGUI[20] suite of programs. The reliability factor $R_w$ was used to assess the quality of the refinement.

To model the local structure in real space, the experimental PDF was extracted from the total scattering data using the program PDFGetN.[21] Background contributions were subtracted and the data were corrected for detector dead-time, absorption, multiple scattering, and inelasticity effects. The data were also normalized by the incident flux and total sample scattering cross-section. The maximum $Q$ vector used for the extraction was 38 Å$^{-1}$. PDF refinements were carried out using the PDFfit program.[22] This program assesses goodness of fit through an $R$ factor representing the difference between observed $G_i^{obs}$ and calculated $G_i^{calcd}$ data points, much like in Rietveld analysis.

Density functional theory calculations were performed using the Cambridge Serial Total Energy Package (CASTEP) as embodied in Accelrys Materials Studio.[23] Norm-conserving nonlocal pseudopotentials were generated using the Kerker scheme with a kinetic energy cutoff of 400 eV. A convergence criterion of 0.00002 eV was applied for the energy change per atom, 0.001 Å for the root-mean-square atomic displacement, and 0.05 eV Å$^{-1}$ for the root-mean-square residual force on movable atoms. Electron exchange and correlation were described using the Perdew−Wang (PW91) generalized gradient approximation (GGA).[24] Geometry optimization utilized the Broyden−Fletcher−Goldfarb−Shanno scheme[25]

(12) Ravel, B.; Kim, Y.-I.; Woodward, P. M.; Fang, C. M. *Phys. Rev. B* **2006**, *73*, 184121.
(13) Dianoux, A.-J.; Lander, G., *Neutron Data Booklet*, 2nd ed.; Institut Laue-Langevin: Grenoble, France, 2003.
(14) Proffen, Th.; Petkov, V.; Billinge, S. J. L.; Vogt, T. *Z. Kristallogr.* **2002**, *217*, 47−50.
(15) Egami, T.; Dmowski, W.; Akbas, M.; Davies, P. K. *AIP Conf. Proc.* **1998**, *436*, 1.
(16) Egami, T.; Teslic, S.; Dmowski, W.; Viehland, D.; Vakhrushev, S. *Ferroelectrics* **1997**, *199*, 103−113.
(17) Petkov, V.; Gateshki, M.; Niederberger, M.; Ren, Y. *Chem. Mater.* **2006**, *18*, 814−821.
(18) Egami, T.; Billinge, S. J. L. *Underneath the Bragg Peaks: Structural Analysis of Complex Materials*: Pergamon Press: Oxford, U.K., 2003.
(19) Proffen, Th.; Egami, T.; Billinge, S. J. L.; Cheetham, A. K.; Louca, D.; Parise, J. B. *Appl. Phys. A* **2002**, *74*, S163.
(20) Larson, A. C.; Von Dreele, R. B. *General Structure Analysis System*; Los Alamos National Laboratory Report LAUR 86-748; Los Alamos National Laboratory: Los Alamos, NM, 1994. Toby, B. H. *J. Appl. Crystallogr.* **2001**, *34*, 210.
(21) Peterson, P. F.; Gutmann, M.; Proffen, Th.; Billinge, S. J. L. *J. Appl. Crystallogr.* **2000**, *33*, 1192.
(22) Proffen, Th.; Billinge, S. J. L. *J. Appl. Crystallogr.* **1999**, *32*, 572−575.
(23) Segall, M. D.; Lindan, P. J. D.; Probert, M. J.; Pickard, C. J.; Hasnip, P. J.; Clark, S. J.; Payne, M. C. *J. Phys.: Condens. Matter* **2002**, *14*, 2717−2744.
(24) Perdew, J. P.; Chevary, J. A.; Vosko, S. H.; Jackson, K. A.; Pederson, M. R.; Singh, D. J.; Fiolhais, C. *Phys. Rev. B* **1992**, *46*, 6671- 6687.
(25) Pfrommer, B. G.; Cote, M.; Louis, S. G.; Cohen, M. L. *J. Comput. Phys.* **1997**, *131*, 133- 140.

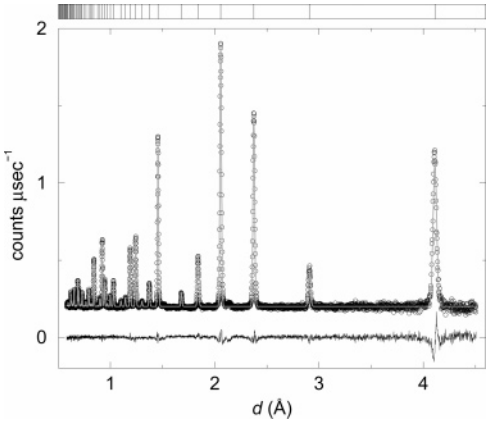


**Figure 1.** Rietveld fit of the time-of flight neutron diffraction data. Experimental data are circles and the solid line is the fit to the average $Pm\bar{3}m$ structure. The difference curve is displayed at the bottom of the plot. Vertical lines in the top panel indicate expected peak positions.

**Table 1. Rietveld and PDF Refinement Results to the Long-Range (average) Structure Using Cubic Space Group $Pm\bar{3}m$; Two *r*-Range Refinements are Reported for the PDF: One Terminating at 10 Å and the Other at 20 Å (note that the reliability factors, $R_w$, for Rietveld refinement and for the PDF cannot be directly compared)**

| | Rietveld | PDF to 10 Å | PDF to 20 Å |
|---|---|---|---|
| *a* (Å) | 4.1103(1) | 4.113(2) | 4.1128(1) |
| $O_{occ}$ | 0.687(5) | | |
| $N_{occ}$ | 0.313(5) | | |
| $R_w$ (%) | 2.14 | 14.8 | 9.96 |

in a manner which permitted both the lattice parameters and atomic coordinates to be optimized.

## Results and Discussion

**Long-Range (Average) Structure** The cubic perovskite structure $Pm\bar{3}m$ was used as a starting point for all refinements, with complete O/N disordering For the *Q*-space Rietveld refinement, background, scaling, profile parameters, lattice parameters, anion occupancy, and atomic displacement parameters were refined. Figure 1 shows the Rietveld fit to the cubic structure for the bank of data with the largest *d* spacings. All detector banks (four in total) were used in the refinement. The (100) peak at the largest *d*-spacing is not very well fitted by Rietveld. This may reflect shortcomings of assuming complete O/N disorder in the Rietveld model. Key results of the refinement are presented in the first column of Table 1 (complete results are given in the Supporting Information). The results and quality of fit are consistent with the findings of other neutron refinement studies. The occupancy of O and N, constrained to fully occupy the anion site, were refined to 0.687(5) and 0.313(5), respectively.

Real-space refinements began with an analysis of the cubic perovskite structure. The pair distribution function offers the advantage of being able to probe structural correlations at different length scales.[18] Over shorter *r*-ranges, local correlations are distinct. Over longer refinement ranges, these configurations steadily damp out and atom−atom interactions correspond increasingly well to the average structure. We refined the average structure over two ranges: from 1.5 to 10 Å, and from 1.5 to 20 Å. PDF refinement included the scale factor, lattice parameters, quadratic peak sharpening, and isotropic atomic displacement parameters. For $Pm\bar{3}m$, the occupancy of O and N at the cube faces was set to 2/3 and 1/3, respectively, allowing for a direct comparison to lower symmetry models in the study. Results of the $Pm\bar{3}m$ structural refinement are given in Table 1 (and more comprehensively in the Supporting Information). The *a* lattice parameter is slightly larger than the one obtained in the Rietveld refinement. No significant difference between the lattice parameters was observed for the two *r*-ranges. The average $Pm\bar{3}m$ structure is not able to fit short-range correlations very well. The fit to the first 10 Å gave $R_w$ = 14.8%, whereas the fit to 20 Å was significantly improved with $R_w$ = 9.96%. This provides direct evidence for short-range structural correlations that lose coherence over distance.

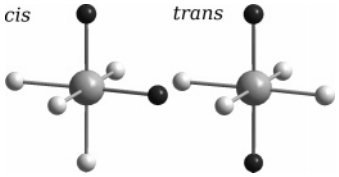


**Figure 2.** cis and trans configurations of the $TaO_4N_2$ octahedron. The central sphere represents Ta, the small dark gray spheres N, and the small light gray spheres O.

**Short-Range (Local) Structure** To analyze the local structure of $BaTaO_2N$ using the PDFfit program, which requires crystallographic descriptions of compounds, we considered several structural models. We report here the detailed analysis of four different models, including the average $Pm\bar{3}m$ crystal structure used in the Rietveld refinement. The models we present here were the most reasonable in terms of their size, the number of refined parameters, and how appropriate they were in describing the essential features of the local structure. It must be emphasized that any superstructure beyond the size of a few perovskite unit cells is too large for a sensible PDF analysis using the tools employed in this work.

The models considered can be classified as cis models where the 2 N on corners of $TaO_4N_2$ octahedron share a common edge, and trans models where N occupy positions on opposite vertices of an octahedron forming linear N−Ta−N bonds. These two configurations are displayed in Figure 2. Furthermore, with respect to Ta displacements (included in the models to account for the asymmetrical environments introduced), unit cells that have a net dipole moment are referred to as polar, whereas antipolar models are those where the dipoles cancel one another. We focused on comparing polar trans, antipolar trans, and antipolar cis structures. We were unsuccessful in constructing a polar cis structure on a reasonable size scale. Larger mixed models, such as those containing cis and trans, or variations of $TaO_{6-m}N_m$ with $m$ = 0, 1, 2, 3, calculated by Fang et al.[11] contain too many atoms for PDF analysis as performed here and were not considered.

The polar trans model allows ions in the average cubic structure to shift along the [001] direction, creating a tetragonal distortion and reducing the symmetry of the cell to $P4mm$. Such a model is displayed in Figure 3a. In the figure, large black Ba atoms occupy the corners of the unit

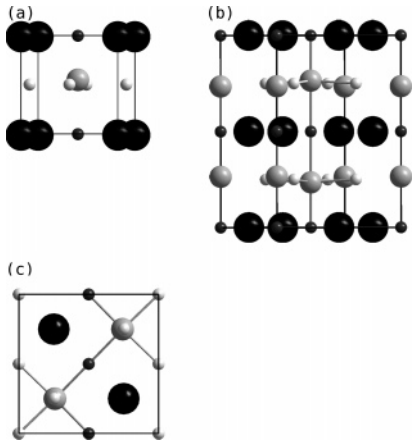


**Figure 3.** Structures considered for this study. Large black spheres are Ba, large gray spheres are Ta, small light gray spheres are O, and small dark gray spheres are N. Ta shifts are exaggerated in the figures for clarity. (a) *P*4*mm* polar trans model, the Ta shift along [001] is evident; (b) *I*4/*mmm* antipolar trans model, two adjacent octahedra have been connected and display opposite directional shifts along [001]; (c) *Pbmm* antipolar cis model, projected down the *c*-axis, the Ta are connected through O and N. Ta shifts toward the N-edges of octahedra.

cell, and large gray Ta atoms are found near the center of the cell. O and N are at the cell faces with dark gray N in a trans arrangement and light gray O in one *xy* plane around the Ta. The Ta shift has been exaggerated in the figure to make the displacement visible.

The antipolar trans model can be envisioned if we again consider a trans arrangement of N and imagine that adjacent octahedra in the structure contain Ta atoms that displace in the opposite direction. In our model in the space group *I*4/*mmm* displayed in Figure 3b, each Ta is allowed to move toward one of its N neighbors, and farther away from the other, along the [001] direction. In Figure 3b, two adjacent octahedra have been connected and the Ta shift has again been exaggerated for clarity.

In the antipolar cis model, N atoms occupy cis positions in the *xy* plane. The structure of the model used, corresponding to space group *Pbmm*, is shown projected down the *c*-axis in Figure 3c. It has linear stripes of N atoms running along the [010] direction. The Ta shift toward the (N-containing) edges of the octahedron, in the $x$ and $-x$ directions, causing the sense of the Ta displacements to cancel. This structure is displayed in greater detail in Figure 4. We have refined the orthorhombic cell with $a = b$, to allow for a comparable number of parameters in the refinement. Other cis structures were considered with more than one Ta plane in the unit cell, but with no improvement to the results.

All models were constructed by ordering O and N on the cubic perovskite lattice as described above. The atom positions were explicitly input into the FINDSYM program of the Isotropy[26] software package in order to obtain the crystallographic descriptions of the ordered structures described here.

Refinement results for these models to 10 Å of *r*, including atomic positions, are given in Table 2. Because PDF results are sensitive to the number of parameters refined, for these different models, positional parameters were refined only when they were found to strongly influence results. In the *P*4*mm* model, Ba was held fixed, but all other ions were allowed to move in the [001] direction. In the two other models, only Ta displacements in specific directions were allowed. The number of refined parameters for each structure are presented in Table 2.

In all cases, the sub-10 Å regime is better fitted with short-range order than it is by the average structure. A PDF refinement using the polar trans *P*4*mm* model results in a sizable improvement over the first 10 Å in real space. $R_w$ improves to 11.9%, compared to 14.8% for the average structure. The results for the antipolar trans *I*4/*mmm* show

(26) Stokes, H. T.; Hatch, D. M. *ISOTROPY*; software and documentation are available over the internet at http://stokes.byu.edu/isotropy.html.

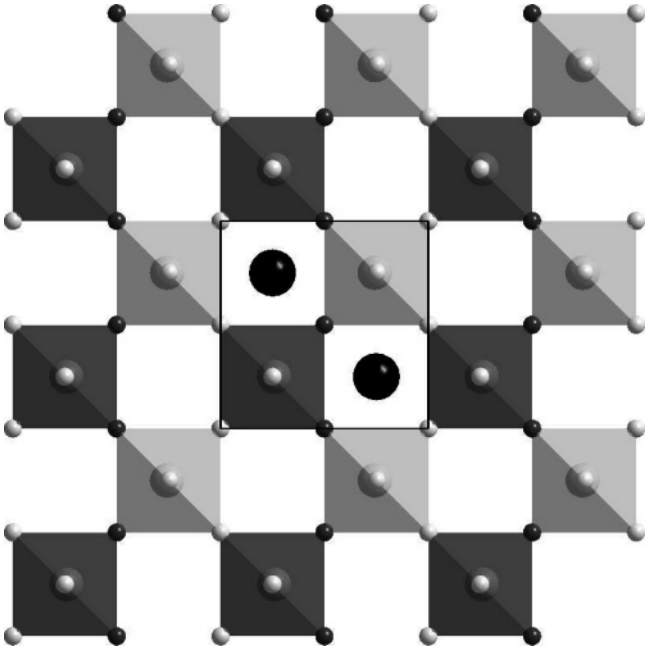

**Figure 4.** Antipolar, cis *Pbmm* structure projected down [001] showing the two kinds of $TaO_4N_2$ polyhedra (dark and light) corresponding to Ta displacements toward $-x$ (light polyhedra) and $+x$ (dark polyhedra). Ba atoms (black spheres) are only displayed within the unit cell, which is outlined.

**Table 2. PDF Refinement Results along with Atomic Positions for the Short-Range $BaTaO_2N$ Structures in the Present Study; Results are for the First 10 Å of *r* (general positions are shown in italics and errors are shown for refined positions) † and ‡ Indicate Atomic Displacement Parameters that were Refined to be the Same.**

| atom | Wyckoff | *x* | *y* | *z* | $U_{iso}$ (Å$^2$) |
|---|---|---|---|---|---|
| | | *P*4*mm* (polar trans)[a] | | | |
| Ba | 1*a* | 0 | 0 | 0 | 0.00661(1) |
| Ta | 1*b* | 0.5 | 0.5 | *0.4877(7)* | 0.00967(1) |
| O | 2*c* | 0.5 | 0 | *0.498(1)* | 0.009029(8) |
| N | 1*b* | 0.5 | 0.5 | *0.002(1)* | 0.00874(1) |
| | | *I*4/*mmm* (antipolar trans)[b] | | | |
| Ba | 4*c* | 0 | 0.5 | 0 | 0.00483(5) |
| Ta | 4*e* | 0 | 0 | *0.7433(7)* | 0.00764(5) |
| O | 8*f* | 0.25 | 0.25 | 0.25 | 0.00819(4) |
| N1 | 2*a* | 0 | 0 | 0 | 0.00734(5)† |
| N2 | 2*b* | 0 | 0 | 0.5 | 0.00734(5)† |
| | | *Pbmm* (antipolar cis)[c] | | | |
| Ba | 2*e* | 0.25 | 0.75 | 0 | 0.00658(2) |
| Ta | 2*f* | *0.254(1)* | 0.25 | 0.5 | 0.00881(2) |
| O1 | 2*b* | 0 | 0 | 0.5 | 0.00744(1)‡ |
| O2 | 2*e* | *0.25* | 0.25 | 0 | 0.00744(1)‡ |
| N | 2*d* | 0.5 | 0 | 0.5 | 0.00696(1) |

[a] $a = 4.1041(3)$ Å, $c = 4.1311(5)$ Å; $R_w = 11.9\%$; 11 parameters. [b] $a = 5.8145(9)$ Å, $c = 8.228(3)$ Å; $R_w = 11.1\%$; 9 parameters. [c] $a = 5.7933(8)$ Å, $c = 4.1411(8)$ Å; $R_w = 9.52\%$; 9 parameters.

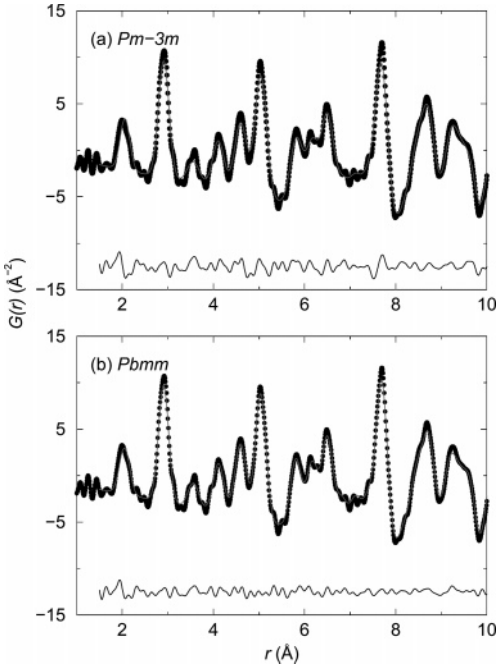


**Figure 5.** Sub-10 Å real space PDF refinement results, corresponding to (a) the average structure $Pm\bar{3}m$ model, and (b) the antipolar cis *Pbmm* structure. Black circles correspond to the experimental PDF and the fits are given as gray lines through the data. The difference curves are presented at the bottom of each panel.

further improvement. $R_w$ improves to 11.1%, while using fewer refinement parameters (9 vs 11 in the previous model). The best model for 1.5 to 10 Å was the antipolar cis model, using *Pbmm*. Here, $R_w$ is 9.52%, also with only 9 refined parameters. Figure 5 shows the experimental PDF fit with the average structure in (a) and the best fit with the *Pbmm* model in (b) to 10 Å.

The difference in the reliability factor between the local structures and the average structure dies out quickly; it is much less significant from 1.5 to 20 Å than from 1.5 to 10 Å. The PDF fit to the polar trans model from 1.5 to 20 Å gave $R_w = 10.6\%$ compared to 9.96% for the average $Pm\bar{3}m$ structure, indicating that distortions of this kind, if present, would have to be very short range. For the antipolar trans and antipolar cis structures, there were slight improvements over the $Pm\bar{3}m$ result, with $R_w = 9.70$ and 8.99%, respectively. Thus, we suggest that the local structure of this $BaTaO_2N$ sample shows a tendency for cis rather than trans $TaO_4N_2$ polyhedra, and the correlation length for this kind of ordering is on the scale of 10 Å.

Table 3 presents bond lengths from the PDF results. In the *P*4*mm* structure, Ta−O and Ta−N bond lengths show a slight shortening of the four equivalent Ta−O bonds (2.0525(3) Å) compared to the $Pm\bar{3}m$ structure (2.0565(1) Å), and one long and one short Ta−N bond arising from the *c*-axis displacements. Bond lengths from the *I*4/*mmm* refinement show Ta−O bonds identical to those in the $Pm\bar{3}m$ structure, and one lengthened and one shortened Ta−N bond. In fact, the bond lengths for the Ta−N bonds are refined to be the same (within error) for both trans models. For the antipolar cis structure, the Ta−O bonds are split into two very similar lengths, at 2.06 and 2.07 Å. Both Ta−N distances are slightly shorter within the octahedra, at 2.03 Å.

DFT calculations provide information on the energetics of different ordered structures, and details of atom positions as a result of geometry optimization. An important distinction between the PDF and DFT results presented here is that in the DFT studies, all general positions were allowed to displace in the geometry optimization, unlike in the PDF refinements, where many general positions were held fixed, and furthermore, *a* and *b* were constrained to be equal in the *Pbmm* structure. A total of seven parameters were refined in this model. Table 4 presents bond lengths from the DFT calculations with corresponding relative energies for the three ordered $BaTaO_2N$ structures. Because the number of formula units per unit cell were not the same for the three structures, the relative energy is expressed per $BaTaO_2N$ formula unit.

The trends (long−medium−short) in the DFT predicted bond lengths agree with those obtained from the PDF refinements for the *P*4*mm* and *Pbmm* models but not for *I*4/*mmm*, although the exact lengths differ. In the *I*4/*mmm* models, the calculated bond lengths are essentially all the same. In the polar trans model (*P*4*mm*), both calculated and experimental values indicate a structural distortion leading to a short Ta−N bond and a long Ta−N bond. However, the difference between long and short bonds is quite large in the calculations, associated with an unusually large *c* parameter. The long−short bond alternation predicted by the calculations effectively lowers the coordination number of the tantalum from octahedral to square pyramidal. This is reminiscent of the structure of $PbVO_3$.[27] In sharp contrast, the two Ta−N bonds are almost identical in the antipolar trans model (*I*4/*mmm*). This can be understood from simple bond valence considerations.[28] In the *P*4*mm* model, each nitrogen makes one short, strong bond with tantalum and one long, weak bond with tantalum. This preserves the net bonding at each nitrogen site. If there were similarly large displacements of the tantalum atoms in the *I*4/*mmm* model, one nitrogen would end up with two short, strong bonds to tantalum and the other nitrogen would end up with two long, weak bonds to tantalum. To avoid this unfavorable local bonding scenario, the structure effectively ends up keeping all six tantalum−anion bonds nearly equidistant. The local distortion calculated for the antipolar cis structure (*Pbmm*) is somewhat larger than the distortion observed from the PDF refinements. This is to be expected given the lack of long-range order in the samples. Nevertheless, the shift of the $Ta^{5+}$ ion toward the edge of the octahedron containing nitrogen is seen both for calculations and experiments. The fact that the calculations show that cis ordering leads to a much smaller local distortion than the polar trans ordering may provide a clue as to why cis ordering is favored in samples where long range anion ordering is absent. The energetics of a structure containing the highly distorted polyhedra associated with polar trans ordering will be very sensitive to the orientation of the resulting square pyramids.

(27) Shpanchenko, R. V.; Chernaya, V. V.; Tsirlin, A. A.; Chizhov, P. S.; Sklovsky, D. E.; Antipov, E. V.; Khlybov, E. P.; Pomjakushin, V.; Balagurov, A. M.; Medvedeva, J. E.; Kaul, E. E.; Geibel, C. *Chem. Mater.* **2004**, *16*, 3267−3273.

(28) Brown, I. D. *The Chemical Bond in Inorganic Chemistry, The Bond Valence Model*; IUCr Monographs on Crystallography 12; Oxford University Press: New York, 2002.

**Table 3. Bond Lengths from PDF Structural Refinements of the Neutron Data, Shown with Reliability Factors for the Models; Refinement Results are for the First 10 Å in Real Space**

| | Rietveld | $Pm\bar{3}m$ | *P*4*mm* | *I*4/*mmm* | *Pbmm* |
|---|---|---|---|---|---|
| $d_{Ta-O}$ (Å) | (4×) 2.05516(6) | (4×) 2.0565(1) | (4×) 2.0525(3) | (4×) 2.0566(5) | (2×) 2.0707(5)<br>(2×) 2.06(1) |
| $d_{Ta-N}$ (Å) | (2×) 2.05516(6) | (2×) 2.0565(1) | (1×) 2.126(7)<br>(1×) 2.005(7) | (1×) 2.112(7)<br>(1×) 2.002(6) | (2×) 2.03(1) |
| $R_w$ (%) | | 14.8 | 11.9 | 11.1 | 9.52 |

**Table 4. Bond Lengths and Relative Energies Per Formula Unit from DFT Calculations of the $BaTaO_2N$ Structures in the Study**

| | *P*4*mm* | *I*4/*mmm* | *Pbmm* |
|---|---|---|---|
| $d_{Ta-O}$ (Å) | (4×) 2.060 | (4×) 2.078 | (2×) 2.176<br>(2×) 2.068 |
| $d_{Ta-N}$ (Å) | (1×) 2.787<br>(1×) 1.870 | (1×) 2.076<br>(1×) 2.075 | (2×) 2.007 |
| $\Delta E$ (meV) | 0 | −482 | −508 |

**Table 5. Bond Lengths and Relative Energies Per Formula Unit from DFT Calculations of Three Different $SrTaO_2N$ Structures**

| | *P*4*mm* | *I*4/*mcm* | *Pbmm* |
|---|---|---|---|
| $d_{Ta-O}$ (Å) | (4×) 2.037 | (4×) 2.059 | (2×) 2.158<br>(2×) 2.036 |
| $d_{Ta-N}$ (Å) | (1×) 2.652<br>(1×) 1.877 | (2×) 2.071 | (2×) 1.993 |
| $\Delta E$ (meV) | 0 | −85 | −550 |

Unlike $PbVO_3$ or $PbTiO_3$, the orientation of the long and short bonds is dependent upon the anion distribution, which presumably does not change much once the compound forms at high temperature. In contrast, the cis geometry preserves a polyhedron whose dimensions are only mildly distorted from an octahedron. Given the lack of long-range N/O order, this would seem to be a more favorable local bonding situation. One interesting result that has not been previously discussed is the fact that for simple ordering schemes, a trans arrangement is needed to generate cooperative displacement that is polar. Therefore, in order to obtain a polar structure that may exhibit ferroelectricity or pyroelectricity it would seem to be essential to find a route to an ordered trans structure. One possible route to stabilizing a trans ordering would be to take advantage of epitaxial lattice matching in thin film architectures to orient the long Ta−N bonds perpendicular to the substrate.

Because $SrTaO_2N$ has been reported to crystallize in a fully ordered structure,[5] we have also performed DFT calculations on this perovskite system, employing three different ordered structures, including the experimentally reported one in the space group *I*4/*mcm*. Table 5 presents bond lengths from the DFT calculations with corresponding relative energies for three $SrTaO_2N$ structures: the trans *P*4*mm*, the reported trans *I*4/*mcm* structure, and the cis *Pbmm* structure, which for $BaTaO_2N$ is calculated to be most stable. For $SrTaO_2N$ as well, it is this *Pbmm* structure, rather than the experimentally reported *I*4/*mcm* trans structure, that is found by DFT to be most stable. Both the *P*4*mm* and the *I*4/*mcm* structure are trans and the former allows short−long N−Ta−N bond alternation, whereas the latter allows tilting of the $TaO_4N_2$ polyhedra. Once again, the *P*4*mm* structure has an unusually large *c* parameter, resulting in nearly square pyramidal Ta. Recent insights on $d^0$ oxide perovskites suggest that when a natural tendency to tilting is frustrated, strong tetragonal off-centering distortions can ensue.[29] Clearly, there is a need for further modeling of these systems using larger supercells that allow both octahedral tilting and bond alternation in trans models.

In conclusion, we have experimentally demonstrated that short-range ordering of O and N exists in $BaTaO_2N$, as the average $Pm\bar{3}m$ structure is unable to capture the local correlations embodied in the sub-10 Å pair distribution function. These local correlations die out quickly over distance, and the average structure is a good model for the 1.5−20 Å PDF. The sub-10 Å PDF is best fitted by an antipolar cis configuration of N in $TaO_4N_2$ octahedra. Further insight is provided by the DFT calculations, which support the experimental conclusion that the cis $TaO_4N_2$ octahedra are more stable.

**Acknowledgment.** K.P. has been supported by the National Science Foundation through a Graduate Student Fellowship. This work was also supported in part by the NSF Chemical Bonding Center CHE 0434567, and by a Career Award (DMR 0449354) to R.S.. The Lujan Center at Los Alamos Neutron Science Center is funded by Department of Energy, Office of Basic Energy Sciences. The upgrade of NPDF at Los Alamos has been funded by the National Science Foundation through Grant DMR 0076488.

**Supporting Information Available:** Three tables with additional information. This material is available free of charge via the Internet at http://pubs.acs.org.

CM0709673

(29) Bilc, D. I.; Singh, D. J. *Phys. Rev. Lett.* **2006**, *96*, 147602(1−4).